Eidgenössische Technische Hochschule Zürich
Swiss Federal Institute of Technology Zurich

Seminar for Applied Mathematics SAM

Time-dependent high-contrast subwavelength resonators

H. Ammari and E.O. Hiltunen

Research Report No. 2021-01
January 2021

Seminar für Angewandte Mathematik
Eidgenössische Technische Hochschule
CH-8092 Zürich
Switzerland

Time-dependent high-contrast subwavelength resonators

Habib Ammari* Erik Orvehed Hiltunen*

Abstract

In the field of metamaterials, many intriguing phenomena arise from having a structure which is periodic in space. In time-dependent structures, conceptually similar properties can arise, which nevertheless have fundamentally different physical implications. In this work, we study time-dependent systems in the context of subwavelength metamaterials. The main result is a capacitance matrix characterization of the band structure, which generalizes previous recent work on static subwavelength metamaterials. Based on this characterization, we numerically compute the dispersion relationship of several time-dependent structures exhibiting interesting wave manipulation properties.

Mathematics Subject Classification (MSC2000): 35J05, 35C20, 35P20.

Keywords: time-dependent materials, subwavelength resonance, subwavelength phononic and photonic crystals.

1 Introduction

The use of so-called metamaterials has been shown to offer extraordinary usability in controlling and manipulating waves. These effects originate from an intricate spatial structure, which is typically repeated periodically in space. A natural generalization of this concept is to consider time-dependent structures, whereby the material parameters depend not only on the spatial variable but are also modulated in time. It is well-known that a "step-like" time-modulation (*i.e.* an instantaneous shift between two constant values) can cause waves to be reflected and refracted, similarly to sharp spatial interfaces between different materials [11, 19, 25, 26]. Moreover, time-modulation provides a way to break reciprocity, which is a fundamental restriction of wave propagation [15, 21, 28, 30, 33].

The case of static materials which are repeated periodically in space has been well-studied using the Floquet-Bloch theory. In particular, we can define a band structure of the material, which describes the frequency-to-momentum relationship of waves inside the material. Crucially, in space-periodic structures, the wave momentum is contained inside the *Brillouin zone*, and is defined modulo elements of the dual lattice. If there is a gap between the band functions, waves with frequencies inside this band gap cannot propagate through the material and will be exponentially decaying.

Inspired by space-periodic structures, it is natural to consider time-modulations which are periodic. Again we can define a band structure, whose frequencies will now be repeated periodically. An interesting application of this is to create frequency-converting systems, which swaps between equivalent frequencies modulo the modulation frequency. Fundamentally, the frequency-conversion is made possible due to the broken energy conservation, which in turn originates from the energy input required to create the time-modulation. Moreover, since there is no energy conservation, there can be unstable waves which are amplified or dampened by the system. In the field of electronics, these ideas have been used to create parametric amplifiers [13]. Unstable Bloch waves are shown as complex frequencies in the band structure, or (restricting to the real Brillouin zone) as band gaps in the momentum variable (known as *momentum*- or *k-gaps*) [12, 17].

Periodic time-modulated structures have been studied in a variety of settings, enabling novel wave phenomena. Due to the energy input, these systems are in general non-Hermitian. This opens the possibility for *exceptional points*, which are parameter points where the eigenmodes coalesce. Such points have a variety of applications, most notably to enhanced sensing [2, 3, 16]. Moreover, the broken time-reversal symmetry can be used to replicate spin effects from quantum systems. As an example, having

*Department of Mathematics, ETH Zürich, Rämistrasse 101, CH-8092 Zürich, Switzerland (habib.ammari@math.ethz.ch, erik.orvehed.hiltunen@sam.math.ethz.ch).

phase-shifted ("rotation-like") modulations can provide a kind of "artificial spin" [14, 18, 32]. These ideas have been used to study classical analogues of the quantum Hall effect, and so-called Floquet topological insulators [14, 27, 29, 31, 32, 35, 36]. In [18], a similar structure was demonstrated to have zero refractive index properties, originating from a linear, cone-like degeneracy in the band structure known as a *Dirac cone* at the origin of the Brillouin zone.

In applications, it is desirable to be able to achieve above mentioned phenomena on *subwavelength* scales. Here, subwavelength means that the length-scale of the system is considerably smaller than the wavelength at which it operates. This is particularly desirable in acoustics, where the wavelengths often are of the order of several meters [23]. Subwavelength metamaterials can be achieved by having a locally resonant microstructure. In other words, the material is composed of building-blocks which themselves are subwavelength resonators [7, 34, 37, 38].

High-contrast resonators is a natural choice of subwavelength resonators when designing subwavelength metamaterials. Here, the subwavelength nature stems from a high material contrast between the constituting materials of the structure, and such structures can be used to achieve a variety of effects [1–5, 7–9]. In this work, we study systems of time dependent high-contrast resonators. The goal is to provide a mathematical foundation that explains effects found in time-modulated systems, for waves in the subwavelength frequency regime. We will begin by carefully defining the notion of subwavelength frequencies in time-modulated systems, which due to the frequency conversion is not immediate to interpret. Afterwards, we will characterize the subwavelength band structure of time-modulated systems of high-contrast resonators.

This work is structured as follows. In Section 2, we formulate the general wave equation problem for time-modulated high-contrast resonators. In the following two sections, we study two different realizations of this problem. In Section 3 we study the case when the time-modulation is applied uniformly in space, both outside and inside the resonators. This can be viewed as a generalization of the problem considered in [17], to systems with more general spatial structures. Similarly to [17], we find that the time-dynamics is governed by the Hill equation, here posed in terms of the instantaneous Minnaert frequencies. We demonstrate that k-gaps can be naturally created this way. Although many interesting phenomena can be realized in such systems, it is impossible to create *e.g.* artificial spin using this type of modulation. Therefore, in Section 4, we consider an alternative time-modulation, applied only to the interior of the resonators. In the asymptotic high-contrast limit, the subwavelength band structure is now characterized by a capacitance matrix formulation, which generalises the case of static systems (see, *e.g.* [5, 8]). In the modulated case, this capacitance matrix formulation is posed as a system of ordinary differential equations in t, which can be viewed as a system of coupled Hill equations. We exemplify this result by numerically computing the band structure of different materials. This way, we demonstrate the possibility of achieving exceptional points and Dirac cones in the subwavelength regime through the use of time-modulation.

2 Problem formulation and preliminary theory

In this section, we define the problem of study. Moreover, we introduce the Floquet-Bloch theory which will be applied in the analysis of the problem.

2.1 Problem formulation

We will solve the wave equation in a structure composed of contrasting materials. The material parameter distribution is given by $\rho(x,t)$ and $\kappa(x,t)$. In the example of acoustic waves ρ and κ correspond to the density and the bulk modulus of the materials. We emphasize, however, that the equation of study is not restricted to acoustic waves but applies to a wider range of classical wave problems, most notably also to polarized electromagnetic waves.

We study the time-dependent wave equation in dimensions $d = 2$ or $d = 3$,

$$\left(\frac{\partial}{\partial t}\frac{1}{\kappa(x,t)}\frac{\partial}{\partial t} - \nabla\cdot\frac{1}{\rho(x,t)}\nabla\right)u(x,t) = 0, \quad x\in\mathbb{R}^d, t\in\mathbb{R}. \tag{2.1}$$

Here, ∇ denotes the gradient with respect to $x \in \mathbb{R}^d$. We assume that the geometry is periodic, as illustrated in Figure 1. Given the linearly independent lattice vectors $l_1, ..., l_d \in \mathbb{R}^d$, we define the lattice Λ and the unit cell Y by

$$\Lambda = \{m_1 l_1 + ... + m_d l_d \mid m_1, ..., m_d \in \mathbb{Z}\}, \qquad Y = \{a_1 l_1 + ... + a_d l_d \mid 0 \le a_1, ..., a_d \le 1\}.$$

We assume that each unit cell contains a system of resonators $D \subset Y$. D is constituted by N domains $D_i, i = 1, ..., N$, each D_i being connected and having boundary of Hölder class $\partial D_i \in C^{1,s}, 0 < s < 1$. The periodic crystal of resonators is then defined by

$$\mathcal{C} = \bigcup_{m \in \Lambda} D + m.$$

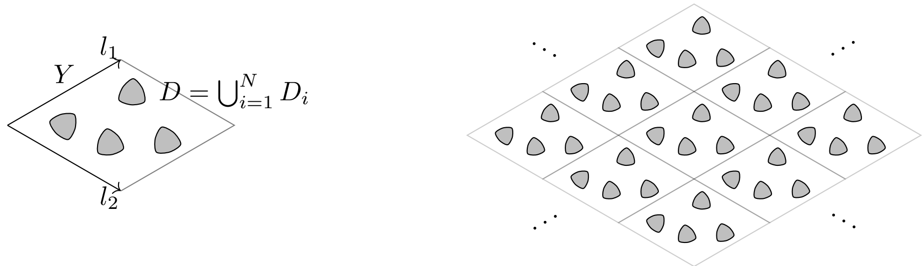

(a) Unit cell Y containing N resonators. *(b) Infinite, periodic system with unit cell Y and lattice Λ.*

Figure 1: Example illustrations of the unit cell and the infinite system of resonators.

In the unmodulated case, the resonators have material parameters κ_b, ρ_b, while the surrounding material has material parameters κ_0, ρ_0. In the modulated case, we will assume that κ and ρ are periodic functions of $t \in \mathbb{R}$, with frequency Ω. We define the static contrast parameter δ and the wave speeds v, v_b as

$$\delta = \frac{\rho_b}{\rho}, \quad v_0 = \sqrt{\frac{\rho_0}{\kappa_0}}, \quad v_b = \sqrt{\frac{\rho_b}{\kappa_b}},$$

and assume that

$$\delta \ll 1, \quad v_0, v_b = O(1).$$

We will consider frequencies ω in the *subwavelength* regime, by which we mean that $\omega \to 0$ as $\delta \to 0$ (typically, in the problems considered here, ω scales as $\omega = O(\delta^{1/2})$).

2.2 Floquet-Bloch theory and quasiperiodic layer potentials

In this section we give a brief introduction to the Floquet-Bloch theory (for further details we refer, for example, to [20]), which is the typical technique used to study differential equations with periodic coefficients. We begin by outlining the theory in the case of ordinary systems of differential equations in the time variable t,

$$y'(t) = A(t)y(t), \quad t \in \mathbb{R}, \tag{2.2}$$

for some $N \times N$ matrix function $A(t)$ which is T-periodic and piecewise continuous in t. If $Y(t)$ denotes the (matrix-valued) fundamental solution, then Floquet's theorem states that there is a constant matrix B such that

$$Y(t) = e^{iBt}P(t),$$

for some T-periodic matrix function P. For each eigenvalue $e^{\mathrm{i}\omega}$ of $e^{\mathrm{i}B}$, there is a *Bloch solution* $y(t)$ satisfying the ω-quasiperiodicity condition that $y(t)e^{-\mathrm{i}\omega t}$ is T-periodic. If e^{iB} is a diagonalizable matrix, there is a basis of Bloch solutions to (2.2). Observe that ω, which we refer to as a *quasifrequency*, is defined modulo $\Omega = \frac{2\pi}{T}$. Therefore, we define the (time-) Brillouin zone $\omega \in Y_t^* := \mathbb{C}/(\Omega\mathbb{Z})$. Observe that we allow complex quasifrequencies. If ω is real, any ω-quasiperiodic function $y(t)$ is bounded in t and is said to be *stable*.

Next, we define analogous concepts in higher dimensions. Given the lattice Λ as defined above, a function $f(x) \in L^2(\mathbb{R}^d)$ is α-quasiperiodic if $e^{-\mathrm{i}\alpha\cdot x}f(x)$ is a Λ-periodic function of x. The quasiperiodicity (or *quasimomentum*) α is defined modulo elements of the *dual lattice* Λ^*, which is the lattice generated by the dual vectors $\alpha_1, ..., \alpha_d$ defined through

$$\alpha_i \cdot l_j = 2\pi\delta_{i,j}, \quad i, j = 1, ..., d.$$

The (space-) *Brillouin zone* Y^* is defined as the torus $Y^* := \mathbb{R}^d/\Lambda^*$. Given a function $f \in L^2(\mathbb{R}^d)$, the Floquet transform is defined as

$$\mathcal{F}[f](x, \alpha) := \sum_{m \in \Lambda} f(x - m)e^{\mathrm{i}\alpha\cdot m}.$$

$\mathcal{F}[f]$ is always α-quasiperiodic in x and periodic in α. The Floquet transform is an invertible map $\mathcal{F}: L^2(\mathbb{R}^d) \to L^2(Y \times Y^*)$ with inverse given by (see, for instance, [6, 20])

$$\mathcal{F}^{-1}[g](x) = \frac{|Y|}{2\pi} \int_{Y^*} g(x, \alpha) \, \mathrm{d}\alpha, \quad x \in \mathbb{R}^d.$$

Applying the Floquet transform in both x and t, we obtain the differential problem

$$\begin{cases} \left(\dfrac{\partial}{\partial t} \dfrac{1}{\kappa(x,t)} \dfrac{\partial}{\partial t} - \nabla \cdot \dfrac{1}{\rho(x,t)} \nabla \right) u(x,t) = 0, \\ u(x,t) e^{-\mathrm{i}\alpha \cdot x} \text{ is } \Lambda\text{-periodic in } x, \\ u(x,t) e^{-\mathrm{i}\omega t} \text{ is } T\text{-periodic in } t. \end{cases} \tag{2.3}$$

For a given $\alpha \in Y^*$, we seek $\omega \in Y_t^*$ such that there is a non-zero solution u to (2.3). At fixed α, such values ω are known to be discrete, $\omega = \omega_n(\alpha)$ for $n = 1, 2, 3....$ The quasifrequencies $\omega_n(\alpha)$, as functions of α, are known as *band functions* and together constitute the band structure, or dispersion relationship, of the material. Observe that the band functions depend continuously on the high-contrast parameter δ.

We remark that the quasifrequencies as defined above can indeed be observed as a generalization of the usual concept of frequency in the unmodulated case. If both κ and ρ are constant in t, we can not define a minimal periodicity T. Requiring (2.3) to hold for any T, we have that $u(x,t)$ is a time-harmonic wave $u(x,t) = v(x)e^{\mathrm{i}\omega t}$ with (ordinary) frequency ω.

For each $n \in \mathbb{Z}^+$, we can represent the (time-) Brillouin zone Y_t^* by the n^{th} Brillouin zone $Y_t^{*,n}$, which is a union of two strips:

$$Y_t^{*,n} = \left[-\frac{n\Omega}{2}, -\frac{(n-1)\Omega}{2} \right) \times \mathrm{i}\mathbb{R} \cup \left[\frac{(n-1)\Omega}{2}, \frac{n\Omega}{2} \right) \times \mathrm{i}\mathbb{R}.$$

We can think of the collection of the n^{th} Brillouin zones as a lifting of the Brillouin zone Y_t^* to $\mathbb{C}$. Since $e^{-\mathrm{i}\omega t} u(x,t)$ is T-periodic in t we have a Fourier series expansion as

$$u(x,t) = e^{\mathrm{i}\omega t} \sum_{n=-\infty}^{\infty} v(x,n) e^{\mathrm{i}n\Omega t}.$$

Although the quasifrequencies ω are defined modulo Y_t^*, choosing a different representation of ω amounts to a re-indexing of the Fourier coefficients $v(x,n)$. This provides a way to associate, at least intuitively, each ω to a certain n^{th} Brillouin zone, where n is chosen to (in some sense) minimise the oscillations of the Fourier series part of u. This idea will be utilized in a precise manner in Definition 2.1 below.

Due to the periodic nature of Y_t^*, the usual definition of subwavelength frequencies does not apply to quasifrequencies. For example, in the particular case when $\Omega = O(\delta^{1/2})$ (which we will sometimes use below), the whole Brillouin zone scales as $O(\delta^{1/2})$ but will typically contain an infinite number of quasifrequencies which originate from folding of non-subwavelength frequencies. Due to this, we introduce the following definition.

Definition 2.1. A quasifrequency $\omega = \omega(\delta) \in Y_t^*$ of (2.3) is said to be a *subwavelength quasifrequency* if there is a corresponding Bloch solution $u(x,t)$, depending continuously on δ, which can be written

$$u(x,t) = e^{\mathrm{i}\omega t} \sum_{n=-\infty}^{\infty} v(x,n) e^{\mathrm{i}n\Omega t},$$

where

$$\omega \to 0 \text{ and } M\Omega \to 0 \text{ as } \delta \to 0,$$

for some integer-valued function $M = M(\delta)$ such that, as $\delta \to 0$, we have

$$\sum_{n=-\infty}^{\infty} \|v(\cdot, n)\|_{L^2(Y)} = \sum_{n=-M}^{M} \|v(\cdot, n)\|_{L^2(Y)} + o(1).$$

In other words, a quasifrequency is a subwavelength quasifrequency if the corresponding Bloch solution only contains components which are either very small, or are in the subwavelength frequency regime. In the static case, we can choose $M = 0$ and obtain the usual definition of a subwavelength frequency.

3 Uniformly modulated high-contrast resonators

In this section, we study the case when the modulation is applied uniformly in space. In other words, the modulation occurs both outside and inside the resonators. We assume that the material parameters are modulated by some envelopes κ_t, ρ_t as follows:

$$\kappa(x,t) = \kappa_x(x)\kappa_t(t), \qquad \rho(x,t) = \rho_x(x)\rho_t(t), \tag{3.1}$$

where the spatial parts κ_x and ρ_x are given by the static parameters:

$$\kappa_x(x) = \begin{cases} \kappa_0, & x \in \mathbb{R}^d \setminus \overline{\mathcal{C}}, \\ \kappa_b, & x \in \mathcal{C}, \end{cases} \qquad \rho_x(x) = \begin{cases} \rho_0, & x \in \mathbb{R}^d \setminus \overline{\mathcal{C}}, \\ \rho_b, & x \in \mathcal{C}. \end{cases} \tag{3.2}$$

We seek solutions to (2.3) by separation of variables. We assume $u(x,t) = \Phi(t)v(x)$ and find that

$$\begin{cases} \dfrac{\mathrm{d}}{\mathrm{d}t}\dfrac{1}{\kappa_t(t)}\dfrac{\mathrm{d}}{\mathrm{d}t}\Phi(t) + \dfrac{\lambda}{\rho_t(t)}\Phi(t) = 0, \\ \Phi(t)e^{-\mathrm{i}\omega t} \quad \text{is } T\text{-periodic}, \end{cases} \tag{3.3}$$

and

$$\begin{cases} \Delta v + \dfrac{\lambda\rho_0}{\kappa_0}v = 0 & \text{in } \mathbb{R}^d \setminus \overline{\mathcal{C}}, \\ \Delta v + \dfrac{\lambda\rho_b}{\kappa_b}v = 0 & \text{in } \mathcal{C}, \\ v|_+ - v|_- = 0 & \text{on } \partial\mathcal{C}, \\ \delta\dfrac{\partial v}{\partial\nu}\Big|_+ - \dfrac{\partial v}{\partial\nu}\Big|_- = 0 & \text{on } \partial\mathcal{C}, \\ v(x)e^{-\mathrm{i}\alpha\cdot x} & \text{is } \Lambda\text{-periodic}, \end{cases} \tag{3.4}$$

for some constant λ. Here, we have interpreted (2.1) in a weak sense, which leads to the so-called *transmission conditions* posed on $\partial\mathcal{C}$ in (3.4). We denote the band functions of the static equation (3.4) by $\omega_{\mathrm{s},i}^\alpha$ for $i = 1,2,\ldots$. In other words, at $\lambda = \left(\omega_{\mathrm{s},i}^\alpha\right)^2$ the equation (3.4) admits a non-zero solution. It is well-known that the first $2N$ band functions scale as $O(\delta^{1/2})$ and are thereby in the subwavelength regime for small δ (N of these band functions have positive real part). Moreover, for small δ, there are explicit asymptotic expansions of these subwavelength band functions (see, for example, [5, 7]).

Substituting $\Phi(t) = \sqrt{\kappa_t(t)}\Psi(t)$ in (3.3), we obtain the following result.

Proposition 3.1. *Assume that the material parameters are given by* (3.1) *and* (3.2). *Then, the quasifrequencies* $\omega = \omega(\alpha) \in Y_t^*$ *to the wave equation* (2.1) *are given by the quasifrequencies of the Hill equation*

$$\Psi''(t) + \left((\omega_i^\alpha(t))^2 + \frac{\sqrt{\kappa_t}}{2}\frac{\mathrm{d}}{\mathrm{d}t}\frac{\kappa_t'}{\kappa_t^{3/2}} \right)\Psi(t) = 0,$$

for $i = 1,2,\ldots$. *Here,* $\omega_i^\alpha(t)$ *are the instantaneous resonance frequencies defined by* $\omega_i^\alpha(t) = \omega_{\mathrm{s},i}^\alpha\sqrt{\frac{\kappa_t(t)}{\rho_t(t)}}$ *for* $\alpha \in Y_s^*$.

Remark 3.2. Proposition 3.1 shows that the band structure of the modulated system is specified by a Hill equation in terms of the band structure of the static system. In particular, the static and modulated systems will have the same degeneracies (modulo Ω). This limits the range of possible phenomena that can be induced with the uniform modulation specified in (3.1), and in Section 4 we consider a different type of modulation which can induce richer phenomena.

3.1 Sinusoidal time-modulation

In this section, we study consequences of Proposition 3.1 in the case when the modulation is sinusoidal with some amplitude ε and frequency Ω.

3.1.1 Modulation of ρ

We begin by studying the case

$$\kappa_t(t) = 1, \qquad \rho_t(t) = \frac{1}{1+\varepsilon\cos(\Omega t)}, \quad 0 \le \varepsilon < 1.$$

Then, setting

$$\tau = \frac{\Omega t}{2}, \qquad a = \left(\frac{2\omega_{\mathrm{s},i}^\alpha}{\Omega}\right)^2, \qquad q = -2\varepsilon\left(\frac{\omega_{\mathrm{s},i}^\alpha}{\Omega}\right)^2,$$

we obtain the equation

$$\phi''(\tau) + (a - 2q\cos(2\tau))\phi(\tau) = 0, \tag{3.5}$$

where ϕ is defined as $\phi(\tau) = \Psi(t)$. Equation (3.5) is known as *Mathieu's equation*, and the quasifrequencies ν of this equation are known as the *characteristic exponents*. Observe that ν and ω are related as

$$\omega = \frac{\Omega\nu}{2}.$$

In the limit as $\delta \to 0$, the behaviour is fundamentally dependent on how ε and Ω scale with δ. In particular, some cases allow complex band functions (*i.e.* unstable solutions, or k-gaps). Crucially, we always have $|q| < a/2$, which suggests that complex bands occur around points where $\omega_{\mathrm{s},i}^\alpha$ is close to $\frac{n\Omega}{2}, n \in \mathbb{Z}$ [24]. As $\delta \to 0$, the subwavelength quasifrequencies are the quasifrequencies associated to the subwavelength static frequencies $\omega_{\mathrm{s},i}^\alpha$ which scale as $O(\delta^{1/2})$.

Case (i): $\varepsilon = o(1)$ as $\delta \to 0$.

In this case, we have that $q/a = o(1)$. From the theory of Mathieu's equation, we have that [24]

$$\nu = \pm\sqrt{a}\big(1 + o(1)\big).$$

It follows that, to leading order, the band structure $\omega(\alpha)$ coincides with the unmodulated case: $\omega(\alpha) = \omega_{\mathrm{s},i}^\alpha + o(1)$.

Case (ii): $\Omega = O(\delta^{1/2})$ and ε is fixed as $\delta \to 0$.

In this case, we have that Ω and $\omega_{\mathrm{s},i}^\alpha$ have the same scaling in δ, and so $a, q = O(1)$. Choosing Ω within the band region of the static problem, we expect complex band functions. Notably, to create a subwavelength k-gap, we require all subwavelength quasifrequencies to be complex. In the case $N = 1$, *i.e.* a single resonator inside the unit cell, both subwavelength bands will open into k-gaps around the same point (as in Figure 3c below). In the case of multiple resonators, $N > 1$, a k-gap can be achieved by centring the complex frequencies around a degeneracy of the static problem (as in Figure 5c below).

Case (iii): Ω and ε are fixed as $\delta \to 0$.

In this case we have $a, q = O(\delta)$, which implies that $\nu = O(\delta^{1/2})$. Consequently, there will be subwavelength quasifrequencies $\omega = O(\delta^{1/2})$, even though Ω is constant. For a, q around 0 and $a > 0$, the Bloch solutions are stable [24] and there are no k-gaps in this case.

Remark 3.3. We can alternatively study the case of step-like changes in the material parameters, where ρ_t changes between the values ρ_1 and ρ_2 at time t_0. Instead of the Mathieu equation, we obtain in this case the Meissner equation,

$$\Psi''(t) + \left(\omega_i^\alpha(t)\right)^2 \Psi(t) = 0, \qquad \omega_i^\alpha(t) = \begin{cases} \dfrac{\omega_{\mathrm{s},i}^\alpha}{\sqrt{\rho_1}}, & -\frac{\Omega}{2} < t < t_0, \\ \dfrac{\omega_{\mathrm{s},i}^\alpha}{\sqrt{\rho_2}}, & t_0 < t < \frac{\Omega}{2}, \end{cases}$$

analogously to [17] but now posed in terms of the instantaneous resonant frequencies $\omega_i^\alpha(t)$.

3.1.2 Modulation of ρ and κ

Here, we briefly mention the case when sinusoidal modulation is applied to both ρ and κ. We assume

$$\kappa_t(t) = \frac{1}{1+\varepsilon\cos(\Omega t)}, \qquad \rho_t(t) = \frac{1}{1+\varepsilon\cos(\Omega t)}, \quad 0 \le \varepsilon < 1.$$

From Proposition 3.1 we then find

$$\Psi'' + \left((\omega_i^\alpha)^2 + \frac{\varepsilon\Omega^2}{2\left(1+\varepsilon\cos(\Omega t)\right)^2}\left(\cos(\Omega t) + \frac{\varepsilon}{4}\left(3+\cos(2\Omega t)\right)\right)\right)\Psi = 0.$$

In general, we cannot obtain the quasifrequencies of this Hill equation in closed form. Nevertheless, under the assumption that $\varepsilon = o(1)$, to leading order we obtain Mathieu equation

$$\phi''(\tau) + (a - 2q\cos(2\tau))\phi(\tau) = 0, \quad \text{where} \quad \tau = \frac{\Omega t}{2}, \quad \phi(\tau) = \Psi(t), \quad a = \left(\frac{2\omega_{s,i}^\alpha}{\Omega}\right)^2, \quad q = -\varepsilon.$$

Now we consider the limit as $\delta \to 0$. If $\Omega = O(\sqrt{\delta})$, we have $q/a = o(1)$, as in Case (i) of the previous section. However, if Ω is fixed and $\varepsilon = O(\delta)$, we have $a, q = O(\delta)$, which corresponds to Case (iii) in the previous section.

3.2 Numerical computations

Here, and throughout this work, we perform the computations in a two-dimensional structure with circular resonators of radius $R = 0.1$ with static material parameters $\rho_0 = \kappa_0 = 1, \rho_b = \kappa_b = 9000$. In this section we compute the band structure in the case

$$\kappa_t(t) = 1, \qquad \rho_t(t) = \frac{1}{1+\varepsilon\cos(\Omega t)}, \quad 0 \leq \varepsilon < 1,$$

for two different geometries. Here, the static band structure $\omega_{s,i}$ is computed using the multipole method as in [7, Appendix C].

3.2.1 Square lattice of resonators

We begin by considering resonators in a square lattice defined through the lattice vectors

$$l_1 = \begin{pmatrix}1\\0\end{pmatrix}, \quad l_2 = \begin{pmatrix}0\\1\end{pmatrix}.$$

The lattice and corresponding Brillouin zone is illustrated in Figure 2. The symmetry points in Y^* are given by $\Gamma = (0,0)$, $\mathrm{M} = (\pi,\pi)$ and $\mathrm{X} = (\pi, 0)$.

The static subwavelength band structure of the system is illustrated in Figure 3a. Although often restricted to positive frequencies, the band structure is symmetric around $\omega = 0$. Figure 3b shows the same band structure, but folded around the frequency $\Omega = 0.2$, which is the same frequency as in Figure 3c where modulation occurs with $\varepsilon = 0.3$. When the modulation is introduced, the frequencies at the edges of the Brillouin zone open into k-gaps.

3.2.2 Honeycomb lattice of resonators

Next, we illustrate the case of a honeycomb lattice of resonators, illustrated in Figure 4. The lattice vectors are given by

$$l_1 = \begin{pmatrix}3\\\sqrt{3}\end{pmatrix}, \quad l_2 = \begin{pmatrix}3\\-\sqrt{3}\end{pmatrix}$$

and the unit cell contains two resonators D_1 and D_2 centred around $c_1 = (1,0)$ and $c_2 = (2,0)$, respectively. The symmetry points in Y^* are given by $\Gamma = (0,0)$, $\mathrm{M} = \alpha_1/2$ and $\mathrm{X} = 2\alpha_1/3 + \alpha_2/3$.

Figure 5 shows the modulated subwavelength band structure for different values of Ω, when $\varepsilon = 0.2$ is fixed. Figure 5a shows $\Omega = 0.3$. In this case, the static band structure is not folded and the modulated band structure is qualitatively similar to the static case. Figure 5b shows $\Omega = 0.23$, where complex frequencies occur. However, some bands remain real and there is no full k-gap. Figure 5c shows the band structure at $\Omega = 0.2$, where all band functions are complex at $\alpha = \mathrm{K}$ and thus exhibit a k-gap.

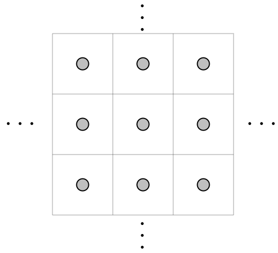

(a) Circular resonators in square lattice.

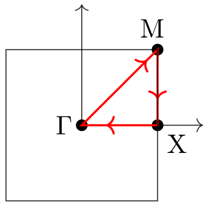

(b) Brillouin zone and the symmetry points Γ, X *and* M.

Figure 2: Illustration of the square lattice, and corresponding Brillouin zone. The red path shows the points where the band functions are computed in Figure 3.

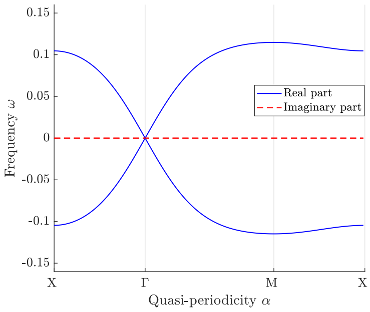

(a) Subwavelength bands in the unmodulated case.

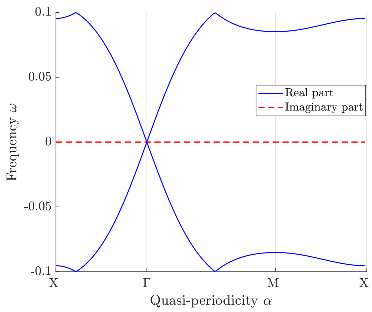

(b) Same as Figure 3a but folded with $\Omega = 0.2$.

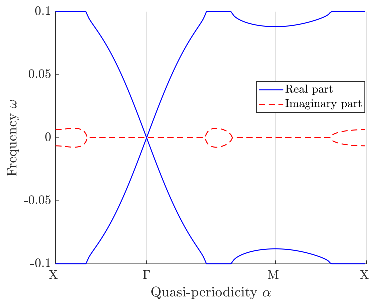

(c) ρ*-modulated structure with* $\Omega = 0.2$ *and* $\varepsilon = 0.3$.

Figure 3: Band structure of high-contrast resonators in a square lattice. As the modulation increases, k-gaps open around the edges of the time-Brillouin zone $[-\Omega/2, \Omega/2)$.

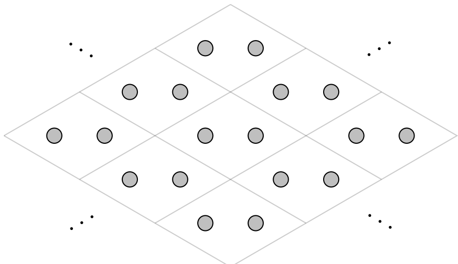

(a) Infinite, periodic system with dimers in a square lattice.

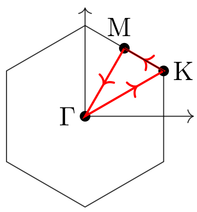

(b) Brillouin zone and the symmetry points Γ, K *and* M.

Figure 4: Illustration of the honeycomb lattice of resonators, and corresponding Brillouin zone. The red path shows the points where the band functions are computed in Figure 5.

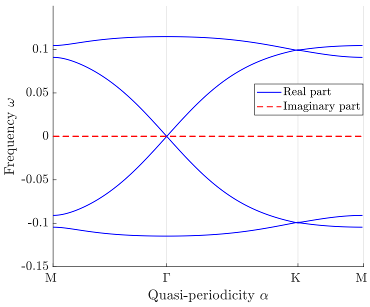

(a) $\varepsilon = 0.2$ *and* $\Omega = 0.3$*, showing largely unaltered band structure compared to static case.*

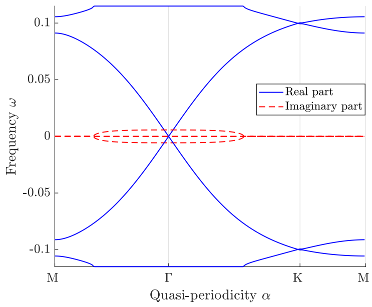

(b) $\varepsilon = 0.2$ *and* $\Omega = 0.23$*, showing complex band frequencies but no full k-gap.*

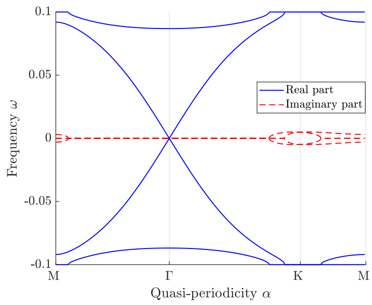

(c) $\varepsilon = 0.2$ *and* $\Omega = 0.2$*, showing a k-gap around the symmetry point* K *in the Brillouin zone.*

Figure 5: Band structure of high-contrast resonators in a honeycomb lattice. For a fixed modulation strength ε*, complex band frequencies may appear for certain* Ω*. A k-gap opens when the degenerate static frequencies become complex (Figure 5c).*

4 Resonator-modulated systems

In this section, we study the case when the time-modulation is only applied to the interior of the resonators, while the surrounding material is constant in time. Due to the time-modulation, we will obtain a system of coupled Helmholtz equations in the frequency domain, posed at frequencies which differ by multiples of Ω.

We consider the periodic structure $\mathcal{C}$ as defined in Section 2.1 and now assume

$$\kappa(x,t) = \begin{cases} \kappa_0, & x \in \mathbb{R}^d \setminus \overline{\mathcal{C}}, \\ \kappa_b \kappa_i(t), & x \in \mathcal{C}_i, \end{cases}, \qquad \rho(x,t) = \begin{cases} \rho_0, & x \in \mathbb{R}^d \setminus \overline{\mathcal{C}}, \\ \rho_b \rho_i(t), & x \in \mathcal{C}_i. \end{cases} \tag{4.1}$$

The functions $\rho_i(t)$ and $\kappa_i(t)$ describe the modulation inside the i^{th} resonator, and we assume that each ρ_i, κ_i is periodic with period Ω. Moreover, we assume that $\kappa_i \in C^1(\mathbb{R})$ and $\kappa_i'(t) = O(\delta^{1/2})$ for each $i = 1, ..., N$.

In Section 4.2, we prove the capacitance matrix approximation of the subwavelength band structure in the limit as $\delta \to 0$. As we shall see, the dynamics is now governed by a system of coupled Hill differential equations in t. We begin, however, by describing the layer potential techniques that will be used in the analysis.

4.1 Layer potential theory and the capacitance matrix

Define the α-quasiperiodic Green's function $G^{\alpha,k}(x,y)$ to satisfy

$$\Delta_x G^{\alpha,k}(x,y) + k^2 G^{\alpha,k}(x,y) = \sum_{n\in\Lambda} \delta(x-n) e^{\mathrm{i}\alpha\cdot n}.$$

If $k \neq |\alpha + q|$ for all $q \in \Lambda^*$, it can be shown [6, 10] that $G^{\alpha,k}$ is given by

$$G^{\alpha,k}(x,y) = \frac{1}{|Y|} \sum_{q\in\Lambda^*} \frac{e^{\mathrm{i}(\alpha+q)\cdot(x-y)}}{k^2 - |\alpha+q|^2}.$$

Let $D \subset \mathbb{R}^d$ be as in Section 2.1. We define the quasiperiodic single layer potential $\mathcal{S}_D^{\alpha,k} : L^2(\partial D) \to H^1_{\text{loc}}(\mathbb{R}^d)$ by

$$\mathcal{S}_D^{\alpha,k}[\phi](x) := \int_{\partial D} G^{\alpha,k}(x,y)\phi(y)\,\mathrm{d}\sigma(y), \quad x \in \mathbb{R}^d.$$

Here, the space $H^1_{\text{loc}}(\mathbb{R}^d)$ consists of functions that are square integrable and with a square integrable weak first derivative, on every compact subset of $\mathbb{R}^d$. Taking the trace on ∂D, it is well-known that $\mathcal{S}_D^{\alpha,0} : L^2(\partial D) \to H^1(\partial D)$ is invertible if $\alpha \neq 0$ [6]. Moreover, on the boundary ∂D, $\mathcal{S}_D^{\alpha,k}$ satisfies the so-called *jump relations*

$$\mathcal{S}_D^{\alpha,k}[\phi]\big|_+ = \mathcal{S}_D^{\alpha,k}[\phi]\big|_-, \tag{4.2}$$

and

$$\frac{\partial}{\partial \nu}\mathcal{S}_D^{\alpha,k}[\phi]\Big|_\pm = \left(\pm\frac{1}{2}I + (\mathcal{K}_D^{-\alpha,k})^*\right)[\phi], \tag{4.3}$$

where I is the identity operator, $\partial/\partial\nu_x$ denotes the outward normal derivative at $x \in \partial D$ and $|_{+,-}$ denote the limits from outside and inside D, respectively. Moreover, $(\mathcal{K}_D^{-\alpha,k})^* : L^2(\partial D) \to L^2(\partial D)$ is the quasiperiodic Neumann-Poincaré operator given by

$$(\mathcal{K}_D^{-\alpha,k})^*[\phi](x) := \int_{\partial D} \frac{\partial}{\partial \nu_x} G^{\alpha,k}(x,y)\phi(y)\,\mathrm{d}\sigma(y).$$

For low frequencies, *i.e.* as $\kappa \to 0$, we have the asymptotic expansions

$$\mathcal{S}_D^{\alpha,k} = \mathcal{S}_D^{\alpha,0} + O(k^2), \tag{4.4}$$

and

$$(\mathcal{K}_D^{-\alpha,k})^* = (\mathcal{K}_D^{-\alpha,0})^* + O(k^2). \tag{4.5}$$

Moreover, we have following well-known integration formula (see, for example, [5]),

$$\int_{\partial D_i} \left(\frac{1}{2}I + (\mathcal{K}_D^{-\alpha,0})^*\right)[\phi]\,\mathrm{d}\sigma = \int_{\partial D_i} \phi\,\mathrm{d}\sigma. \tag{4.6}$$

Finally, for $\alpha \neq 0$, the basis functions ψ_i^α and the capacitance coefficients C_{ij}^α are defined as

$$\psi_i^\alpha = \left(\mathcal{S}_D^{\alpha,0}\right)^{-1}[\chi_{\partial D_i}], \qquad C_{ij}^\alpha = -\int_{\partial D_i} \psi_j^\alpha \,\mathrm{d}\sigma, \tag{4.7}$$

for $i, j = 1, ..., N$. The capacitance matrix C^α is defined as the matrix $C^\alpha = \left(C_{ij}^\alpha\right)$.

4.2 Capacitance matrix formulation of the problem

In this section, we will use the above notion of capacitance in order to derive an asymptotic expansion of the subwavelength band functions as $\delta \to 0$.

We seek solutions to (2.3) under the modulation specified in (4.1). From the regularity of ρ and κ we know that u is continuously differentiable in t [22]. Since $e^{-\mathrm{i}\omega t}u(x,t)$ is a T-periodic in t we have a Fourier series expansion as

$$u(x,t) = e^{\mathrm{i}\omega t}\sum_{n=-\infty}^{\infty} v(x,n)e^{\mathrm{i}n\Omega t}.$$

In the time domain, we have the boundary conditions at $x \in \partial D_i$

$$\delta \frac{\partial u}{\partial \nu}\bigg|_+ - \frac{1}{\rho_i}\frac{\partial u}{\partial \nu}\bigg|_- = 0, \qquad x \in \partial D_i, t \in \mathbb{R}.$$

In the frequency domain, we then have the following equation, for $n \in \mathbb{Z}$:

$$\begin{cases} \Delta v + \dfrac{\rho_0(\omega + n\Omega)^2}{\kappa_0} v = 0 & \text{in } Y \setminus \overline{D}, \\ \Delta v_i^* + \dfrac{\rho_b(\omega + n\Omega)^2}{\kappa_b} v_i^{**} = 0 & \text{in } D_i, \\ v|_+ - v|_- = 0 & \text{on } \partial D, \\ \delta \dfrac{\partial v}{\partial \nu}\bigg|_+ - \dfrac{\partial v_i^*}{\partial \nu}\bigg|_- = 0 & \text{on } \partial D_i, \\ v(x,n)e^{\mathrm{i}\alpha\cdot x} \text{ is } \Lambda\text{-periodic in } x. \end{cases} \tag{4.8}$$

Here, $v_i^*(x,n)$ and $v_i^{**}(x,n)$ are defined through the convolutions

$$v_i^*(x,n) = \sum_{m=-\infty}^{\infty} r_i(m)v(x,n-m), \quad v_i^{**}(x,n) = \frac{1}{\omega + n\Omega}\sum_{m=-\infty}^{\infty} k_i(m)\big(\omega + (n-m)\Omega\big)v(x,n-m),$$

where r_i and k_i are the Fourier series coefficients of $1/\rho_i$ and $1/\kappa_i$, respectively:

$$\frac{1}{\rho_i(t)} = \sum_{n=-\infty}^{\infty} r_i(n)e^{\mathrm{i}n\Omega t}, \quad \frac{1}{\kappa_i(t)} = \sum_{n=-\infty}^{\infty} k_i(n)e^{\mathrm{i}n\Omega t}.$$

Observe that (4.8) consists of coupled Helmholtz equations at frequencies differing by integer multiples of Ω. The coupling of the Helmholtz equations is specified through ρ_i and κ_i. Rescaling a solution to (4.8) produces another solution, so we assume that the solution is normalized as $\|v(\cdot,1)\|_{H^1(Y)} = 1$. Since u is continuously differentiable in t, we then have as $n \to \infty$,

$$\|v(\cdot,n)\|_{H^1(Y)} = o\left(\frac{1}{n}\right). \tag{4.9}$$

We will consider the case when the modulation of ρ consists of a finite Fourier series with a large number of nonzero Fourier coefficients:

$$\frac{1}{\rho_i(t)} = \sum_{n=-M}^{M} r_i(n)e^{\mathrm{i}n\Omega t},$$

for some $M \in \mathbb{N}$ satisfying

$$M = O\left(\delta^{-\gamma/2}\right),$$

for some $0 < \gamma < 1$. We seek subwavelength quasifrequencies ω of the wave equation (2.3) in the sense of Definition 2.1. In particular, we assume that ω, and also the frequency Ω of the modulation, is of the same order as the static subwavelength resonant frequencies:

$$\omega = O\left(\delta^{1/2}\right), \qquad \Omega = O\left(\delta^{1/2}\right).$$

We then have the following result.

Lemma 4.1. *As $\delta \to 0$, the functions $v_i^*(x,n)$ are approximately constant for x inside D_i, i.e.,*

$$v_i^*(x,n) = c_i(n) + O(\delta^{(1-\gamma)/2}), \quad x \in D_i,$$

uniformly for $n \le M$, for some constants $c_i(n)$, $i = 1, ..., N$.

Proof. Since v_i^* is defined through a finite convolution, we have from (4.9) that

$$\|v_i^*(\cdot,n)\|_{H^1(Y)} \le \frac{K^*}{n}, \quad n \neq 0,$$

for some constant K^*. For $|n| \le M$ we have from (4.8) that

$$\int_{\partial D_i} v_i^* \frac{\partial v_i^*}{\partial \nu} \, \mathrm{d}\sigma = O(\delta), \qquad \int_{D_i} v_i^* \Delta v_i^* \, \mathrm{d}x = O(\delta^{1-\gamma}).$$

Using integration by parts, we obtain

$$\begin{aligned} \int_{D_i} |\nabla v_i^*|^2 \, \mathrm{d}x &= \int_{\partial D_i} v_i^* \frac{\partial v_i^*}{\partial \nu} \, \mathrm{d}\sigma - \int_{D_i} v_i^* \Delta v_i^* \, \mathrm{d}x \\ &= O(\delta^{1-\gamma}). \end{aligned}$$

Therefore, for $|n| \le M$ we have $v_i^*(x,n) = c_i(n) + O(\delta^{(1-\gamma)/2})$ for $x \in D_i$, which proves the claim. □

In $Y \setminus \overline{D}$, the solution v satisfies the Helmholtz equation and can be represented through the single layer potential as

$$v(x,n) = \mathcal{S}_D^{\alpha,\omega+n\Omega}[\phi_n](x),$$

for some ϕ_n, $n \in \mathbb{Z}$. From (4.9) we have that $\|\phi_n\|_{L^2(\partial D)} \le \widetilde{K}/n$ as $n \to \infty$, for some constant $\widetilde{K}$. Using (4.2) and (4.4) we have on the boundary ∂D_i:

$$\begin{aligned} v_i^*(x,n) &= \sum_{m=-M}^{M} r(m) \mathcal{S}_D^{\alpha,\omega+(n-m)\Omega}[\phi_{n-m}](x) \\ &= \mathcal{S}_D^{\alpha,0}\left[\sum_{m=-M}^{M} r(m)\phi_{n-m}\right](x) + O(\delta^{1-\gamma}), \end{aligned}$$

as $\delta \to 0$, where the error term is uniform for $|n| \le M$. From Lemma 4.1 we then find that

$$\sum_{m=-M}^{M} r(m)\phi_{n-m} = \sum_{i=1}^{N} c_i(n)\psi_i^\alpha + O(\delta^{(1-\gamma)/2}), \tag{4.10}$$

for $\alpha \neq 0$, where ψ_i^α are the basis functions defined in (4.7).

On one hand, using the transmission conditions and integrating by parts, we obtain

$$\int_{\partial D_i} \left.\frac{\partial v(x,n)}{\partial \nu}\right|_+ \mathrm{d}\sigma(x) = \frac{1}{\delta}\int_{\partial D_i} \left.\frac{\partial v_i^*(x,n)}{\partial \nu}\right|_- \mathrm{d}\sigma(x) = -\frac{\rho_b(\omega+n\Omega)^2}{\delta\kappa_b} V_i^{**}(n), \tag{4.11}$$

where $V_i^{**}(n)$ is defined as

$$V_i^{**}(n) = \frac{1}{\omega+n\Omega}\sum_{m=-\infty}^{\infty} k_i(m)\big(\omega+(n-m)\Omega\big)V_i(n-m), \quad V_i(n) = \int_{D_i} v(x,n)\,\mathrm{d}x.$$

On the other hand, using the jump relation, (4.3), the asymptotic expansion (4.5) and the integration formula (4.6) we have

$$\int_{\partial D_i} \frac{\partial v(x,n)}{\partial \nu}\bigg|_+ \mathrm{d}\sigma(x) = \int_{\partial D_i} \left(\frac{1}{2}I + (\mathcal{K}_D^{-\alpha,0})^*\right)[\phi_n]\,\mathrm{d}\sigma + O(\delta^{(1-\gamma)/2}) = \int_{\partial D_i} \phi_n \,\mathrm{d}\sigma + O(\delta^{(1-\gamma)/2}),$$

for $|n| \leq M$. Taking the convolution and using (4.10), we have

$$\sum_{m=-M}^{M} r(m) \int_{\partial D_i} \frac{\partial v(x,n-m)}{\partial \nu}\bigg|_+ \mathrm{d}\sigma(x) = -\sum_{j=1}^{N} c_j(n) C_{ij}^{\alpha} + O(\delta^{(1-\gamma)/2}), \tag{4.12}$$

where C_{ij}^{α} are the capacitance coefficients defined in (4.7). Combining (4.11) and (4.12) we therefore obtain

$$\sum_{j=1}^{N} c_j(n) C_{ij}^{\alpha} = \frac{\rho_b}{\delta \kappa_b} \sum_{m=-M}^{M} r_i(m)(\omega + (n-m)\Omega)^2 V_i^{**}(n-m) + O(\delta^{(1-\gamma)/2}). \tag{4.13}$$

Next we will take the inverse transform of (4.13). Denoting

$$c_i(t) = e^{\mathrm{i}\omega t} \sum_{n=-\infty}^{\infty} c_i(n) e^{\mathrm{i}n\Omega t}, \quad V_i(t) = e^{\mathrm{i}\omega t} \sum_{n=-\infty}^{\infty} V_i(n) e^{\mathrm{i}n\Omega t},$$

we have

$$c_i(t) = \frac{V_i(t)}{|D_i|\rho_i(t)},$$

where $|D_i|$ denotes the volume (or area) of the i^{th} resonator D_i. Assuming that v corresponds to a subwavelength solution, we have as $\delta \to 0$,

$$c_i(t) = e^{\mathrm{i}\omega t} \sum_{n=-M}^{M} c_i(n) e^{\mathrm{i}n\Omega t} + o(1), \quad V_i(t) = e^{\mathrm{i}\omega t} \sum_{n=-M}^{M} V_i(n) e^{\mathrm{i}n\Omega t} + o(1).$$

This together with (4.13) proves the following main result.

Theorem 4.2. *Assume that the material parameters are given by* (4.1) *and that* $\alpha \neq 0$. *Then, as* $\delta \to 0$, *the quasifrequencies* $\omega = \omega(\alpha) \in Y_t^*$ *to the wave equation* (2.1) *in the subwavelength regime are, to leading order, given by the quasifrequencies of the system of ordinary differential equations*

$$\sum_{j=1}^{N} C_{ij}^{\alpha} c_j(t) = -\frac{|D_i|\rho_b}{\delta \kappa_b} \frac{1}{\rho_i(t)} \frac{\mathrm{d}}{\mathrm{d}t}\left(\frac{1}{\kappa_i(t)} \frac{\mathrm{d}\rho_i c_i}{\mathrm{d}t}\right) + o(1), \tag{4.14}$$

for $i = 1, ..., N$.

We remark that the left-hand side of (4.14) is specified by the entries of the matrix-vector product $C^{\alpha}c(t)$. In fact, we can rewrite the leading order of (4.14) into the following system of Hill equations

$$\Psi''(t) + M(t)\Psi(t) = 0, \tag{4.15}$$

where Ψ is the vector defined as

$$\Psi = \left(\frac{\rho_i(t)}{\sqrt{\kappa_i(t)}} c_i(t)\right)_{i=1}^{N}$$

and M is the matrix defined as

$$M(t) = \frac{\delta \kappa_b}{\rho_b} W_1(t) C^{\alpha} W_2(t) + W_3(t),$$

with W_1, W_2 and W_3 being the diagonal matrices with diagonal entries

$$(W_1)_{ii} = \frac{\sqrt{\kappa_i}\rho_i}{|D_i|}, \qquad (W_2)_{ii} = \frac{\sqrt{\kappa_i}}{\rho_i}, \qquad (W_3)_{ii} = \frac{\sqrt{\kappa_i}}{2} \frac{\mathrm{d}}{\mathrm{d}t} \frac{\kappa_i'}{\kappa_i^{3/2}},$$

for $i = 1, ..., N$.

Remark 4.3. If we assume that all resonators have equal volume and that

$$\kappa_i(t) = 1, \quad \text{and} \quad \rho_i(t) = \rho_0(t),\ t \in \mathbb{R}, i = 1,..,N,$$

(in other words that κ is unmodulated and ρ_i are equal for all i), equation (4.15) and the corresponding quasifrequencies ω_i^α read

$$\Psi''(t) + \frac{\delta\kappa_b}{|D_1|\rho_b} C^\alpha \Psi = 0, \qquad \omega_i^\alpha = \sqrt{\frac{\delta\kappa_b\lambda_i^\alpha}{\rho_b|D_1|}},$$

where λ_i^α are the eigenvalues of C^α. This agrees with the formula for the static subwavelength resonant frequencies given in [5], and we remark that this holds even if the system has a nontrivial modulation of ρ specified by ρ_0.

4.3 Numerical computations

We will numerically compute the Floquet exponents of the Hill system of equations

$$\Psi''(t) + M(t)\Psi(t) = 0. \tag{4.16}$$

This is an $N \times N$ system of ordinary differential equations of second order, which admits a fundamental basis of solutions $\{\psi_{\mathrm{I},j}(t), \psi_{\mathrm{II},j}(t)\}_{j=1}^N$ defined through the initial conditions

$$\psi_{\mathrm{I},j}^{(i)}(0) = \delta_{ij}, \quad \left(\psi_{\mathrm{I},j}^{(i)}\right)'(0) = 0, \qquad \psi_{\mathrm{II},j}^{(i)}(0) = 0, \quad \left(\psi_{\mathrm{II},j}^{(i)}\right)'(0) = \delta_{ij}. \tag{4.17}$$

Here, and throughout this section, bracketed superscripts denote corresponding vector components. We seek quasiperiodic solutions ψ satisfying

$$\psi(t+T) = e^{\mathrm{i}\omega T}\psi(t).$$

It is easy to show that this occurs precisely when $e^{\mathrm{i}\omega T}$ is an eigenvalue of the fundamental solution, which is the $2N \times 2N$-matrix

$$\mathcal{W} = \begin{pmatrix} \left(\psi_{\mathrm{I},j}^{(i)}(T)\right)_{i,j=1}^N & \left(\psi_{\mathrm{II},j}^{(i)}(T)\right)_{i,j=1}^N \\ \left(\left(\psi_{\mathrm{I},j}^{(i)}\right)'(T)\right)_{i,j=1}^N & \left(\left(\psi_{\mathrm{II},j}^{(i)}\right)'(T)\right)_{i,j=1}^N \end{pmatrix}.$$

This offers a straightforward numerical algorithm to compute the Floquet exponents ω: we numerically integrate (4.16) with initial conditions (4.17), and then approximate ω through the eigenvalues of $\mathcal{W}$.

4.3.1 Exceptional point degeneracy in square lattice of dimers

We begin by considering the band structure of a structure with the same square lattice as in Section 3.2.1, but where the unit cell now contains two resonators D_1, D_2 centred at $c_1 = (0.5 - 1.2R, 0.5)$, $c_2 = (0.5 + 1.2R, 0.5)$, respectively. The geometry is illustrated in Figure 6. We consider the modulation specified by

$$\rho_1(t) = 1, \quad \rho_2(t) = 1, \quad \kappa_1(t) = \frac{1}{1+\varepsilon\cos(\Omega t)}, \quad \kappa_2(t) = \frac{1}{1+\varepsilon\cos(\Omega t + \pi)}, \qquad t \in \mathbb{R},$$

for $0 \le \varepsilon < 1$. As we will see, this structure may support exceptional points, which (as mentioned in the introduction) are parameter points where the eigenmodes of the system coalesce.

The band structure of the material is given in Figure 7. Figure 7a shows the static band structure (corresponding to $\varepsilon = 0$) folded with $\Omega = 0.26$. This frequency Ω lies inside a band gap, and there are intersections between the first (unfolded) and the second (folded) bands. Figure 7b shows the modulated band structure at $\varepsilon = 0.08$, also with $\Omega = 0.26$. In the modulated structure, the intersection points marks a transition from a real to a conjugate-symmetric spectrum. Considering the eigenvectors, Figure 3c shows that the eigenvector matrix of $\mathcal{W}$ is defective at the degeneracies, and we conclude that the degenerate points correspond to exceptional points.

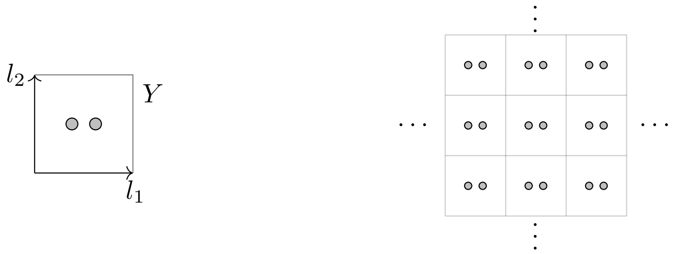

(a) Square unit cell Y containing 2 resonators. *(b) Infinite, periodic system with dimers in a square lattice.*

Figure 6: Illustration of the square lattice of dimers, which may support an exceptional point.

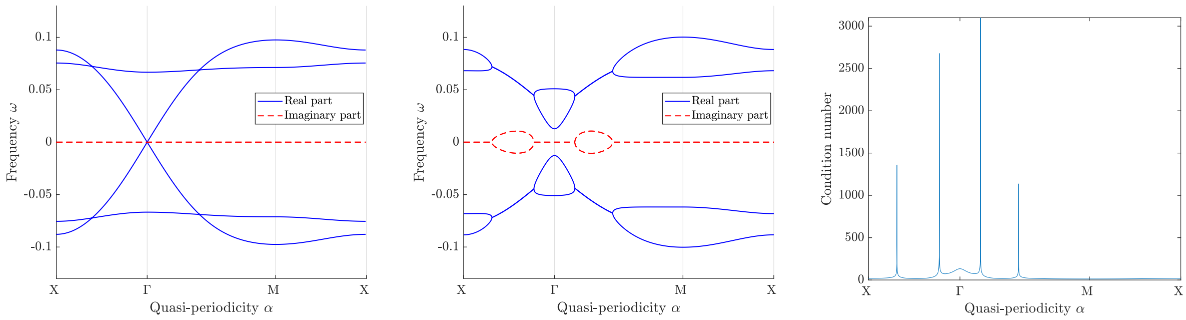

(a) Static band structure of the square lattice of dimers, folded with $\Omega = 0.26$. *(b) $\varepsilon = 0.2$ and $\Omega = 0.26$, showing exceptional point degeneracies at some points in the Brillouin zone.* *(c) Condition number of the eigenvector matrix of $\mathcal{W}$, showing a defective matrix at the degenerate points.*

Figure 7: Band structure of high-contrast dimers of resonators in a square lattice. For nonzero modulation strengths ε, the bands form exceptional point degeneracies where the system is defective and the spectrum changes from being real to being conjugate-symmetric.

4.3.2 Dirac cone degeneracy at Γ in trimer honeycomb lattice

Next, we consider a honeycomb lattice of resonator trimers as illustrated in Figure 8, similar to structures considered in [14, 18]. We use the same lattice as in Section 3.2.2, where the unit cell now contains six resonators D_i respectively centred at c_i, $i = 1, .., 6$, given by

$$c_1 = (1,0) + 3R(1,0), \quad c_2 = (1,0) + 3R\left(\cos\left(\frac{2\pi}{3}\right), \sin\left(\frac{2\pi}{3}\right)\right), \quad c_3 = (1,0) + 3R\left(\cos\left(\frac{4\pi}{3}\right), \sin\left(\frac{4\pi}{3}\right)\right),$$
$$c_4 = (2,0) + 3R\left(\cos\left(\frac{\pi}{3}\right), \sin\left(\frac{\pi}{3}\right)\right), \qquad c_5 = (2,0) - 3R(1,0), \quad c_6 = (2,0) + 3R\left(\cos\left(\frac{5\pi}{3}\right), \sin\left(\frac{5\pi}{3}\right)\right).$$

We use the modulation given by $\kappa_i(t) = 1, \ i = 1, ..., 6$ and

$$\rho_1(t) = \rho_4(t) = \frac{1}{1 + \varepsilon\cos(\Omega t)}, \quad \rho_2(t) = \rho_5(t) = \frac{1}{1 + \varepsilon\cos\left(\Omega t + \frac{2\pi}{3}\right)}, \quad \rho_3(t) = \rho_6(t) = \frac{1}{1 + \varepsilon\cos\left(\Omega t + \frac{4\pi}{3}\right)},$$

for $0 \leq \varepsilon < 1$.

The band structure of the material is presented in Figure 9 with modulation frequency $\Omega = 0.15$. In the static case, the band structure is folded and, as expected, exhibits a Dirac cone at $\alpha = \mathrm{K}$ [5]. As ε increases, the gap between the 4^{th} and the 5^{th} bands at Γ decreases. At a specific point, namely $\varepsilon = 0.3$, the gap closes in a Dirac cone at Γ. We remark that this linear dispersion at the origin of the Brillouin zone is a prerequisite for creating double-zero index materials [9, 17].

5 Concluding remarks

In this work, we have provided a mathematical foundation for time-dependent systems of high-contrast subwavelength resonators. We have considered two types of time-modulation. In the case of uniform time-modulation, the wave equation is separable and the quasifrequency band structure is described as

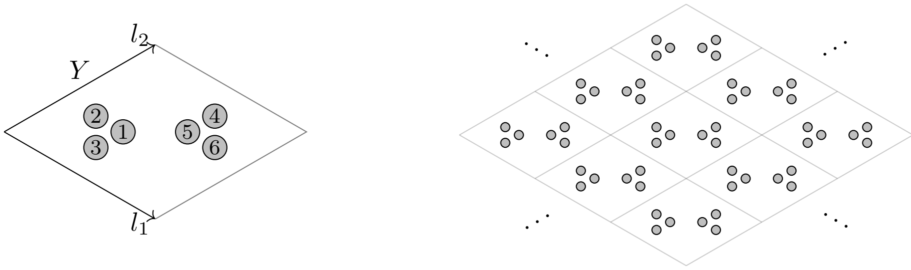

(a) Hexagonal lattice unit cell Y containing 6 resonators. *(b) Periodic system with trimers in a honeycomb lattice.*

Figure 8: Illustration of the "artificial spin" honeycomb lattice, which can support a Dirac cone degeneracy at Γ.

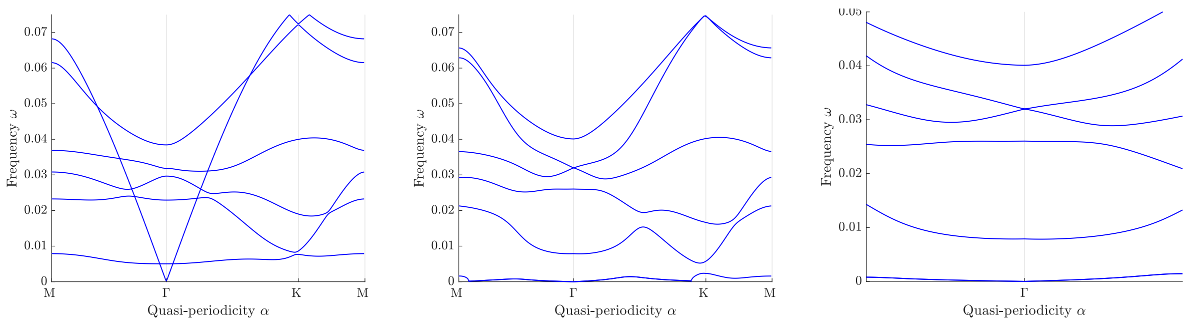

(a) Static, folded, band structure of the honeycomb lattice of trimers. *(b) Modulated band structure at $\varepsilon = 0.3$ and $\Omega = 0.15$, showing Dirac cones at both* Γ *and* K. *(c) Close-up of Figure 9b around Γ, showing the Dirac cone of the 4^{th} and 5^{th} bands.*

Figure 9: Band structure of high-contrast resonators in a trimer honeycomb lattice. The static band structure (Figure 9a) shows a Dirac cone at K. *As the modulation increases, the gap between the 4^{th} and 5^{th} bands closes, and at $\varepsilon = 0.3$ the gap closes in a Dirac cone. For clarity, only the positive real part of the band structure is shown.*

the quasifrequencies of a Hill differential equation in terms of the static band structure. In the case where the time-modulation only occurs inside the resonators, the subwavelength band structure admits a capacitance matrix characterization, which generalizes the recently derived characterization in the static case. We have exemplified both types of modulation numerically, and demonstrated k-gaps, exceptional points and Dirac cone degeneracies at the origin of the Brillouin zone, which is a prerequisite for achieving zero-refractive index materials in the subwavelength regime.

A Finite system of resonators

In this section, we derive the corresponding results in setting of finite resonator systems. We let D be a finite resonator system, defined as in Section 2.1 but not repeated periodically. Again, we compute the quasifrequencies ω of the wave equation (2.1) (we emphasize that there is no quasiperiodic condition in the spatial dimension in this case, and ω represent resonant frequencies and not band functions).

A.1 Uniformly modulated systems

As in Section 3, we assume that the material parameters are modulated by some envelopes κ_t, ρ_t as follows:

$$\kappa(x,t) = \kappa_x(x)\kappa_t(t), \qquad \rho(x,t) = \rho_x(x)\rho_t(t). \tag{A.1}$$

Now, we assume the spatial parts κ_x and ρ_x satisfy

$$\kappa_x(x) = \begin{cases} \kappa_0, & x \in \mathbb{R}^d \setminus \overline{D}, \\ \kappa_b, & x \in D, \end{cases} \qquad \rho_x(x) = \begin{cases} \rho_0, & x \in \mathbb{R}^d \setminus \overline{D}, \\ \rho_b, & x \in D. \end{cases} \tag{A.2}$$

We seek solutions to (2.1) by separation of variables. Assume $u(x,t) = \Phi(t)v(x)$. Then we find from (2.1) that

$$\frac{\mathrm{d}}{\mathrm{d}t}\frac{1}{\kappa_t(t)}\frac{\mathrm{d}}{\mathrm{d}t}\Phi(t) + \frac{\omega^2}{\rho_t(t)}\Phi(t) = 0 \tag{A.3}$$

and

$$\begin{cases} \Delta v + \dfrac{\omega^2\rho_0}{\kappa_0} v = 0 & \text{in } \mathbb{R}^d \setminus \overline{D}, \\ \Delta v + \dfrac{\omega^2\rho_b}{\kappa_b} v = 0 & \text{in } D, \\ v|_+ - v|_- = 0 & \text{on } \partial D, \\ \delta \dfrac{\partial v}{\partial \nu}\Big|_+ - \dfrac{\partial v}{\partial \nu}\Big|_- = 0 & \text{on } \partial D, \end{cases} \tag{A.4}$$

for some constant ω. In the static case, (A.4) is usually coupled with the outgoing Sommerfeld radiation condition, in order to select the physical solution. In the modulated case however, due to lack of energy conservation, there may be both outgoing and incoming solutions. We denote the outgoing (respectively incoming) resonant frequencies by $\omega_{\mathrm{s},i}^+$ (respectively $\omega_{\mathrm{s},i}^-$) for $i = 1, 2, ...$ We observe that $\omega_{\mathrm{s},i}^- = \overline{\omega_{\mathrm{s},i}^+}$. It is well-known that the first $2N$ resonant frequencies scale as $O(\delta^{1/2})$ and N of these have positive real part (known as the *Minnaert frequencies*) [1]. These are real to leading order, and we have $\omega_{\mathrm{s},i}^+ = \omega_{\mathrm{s},i}^- + O(\delta)$ for $i = 1, 2, ..., 2N$. Substituting $\Phi(t) = \sqrt{\kappa_t(t)}\Psi(t)$ we can obtain the following result.

Proposition A.1. *Assume that the material parameters are given by* (A.1) *and* (A.2)*. Then, the quasifrequencies $\omega \in Y_t^*$ to the wave equation* (2.1) *in the subwavelength regime are given by the quasifrequencies of the Hill equation*

$$\Psi''(t) + \left(\left(\omega_i^\pm(t)\right)^2 + \frac{\sqrt{\kappa_t}}{2}\frac{\mathrm{d}}{\mathrm{d}t}\frac{\kappa_t'}{\kappa_t^{3/2}} \right)\Psi(t) = 0,$$

for $i = 1, 2, ...,$. Here, $\omega_i^\pm(t)$ are the instantaneous resonant frequencies defined by $\omega_i^\pm(t) = \omega_{\mathrm{s},i}^\pm \sqrt{\frac{\kappa_t(t)}{\rho_t(t)}}$.

A.2 Resonator-modulated systems

We now consider the finite analogue of the system studied in Section 4. For simplicity, we will restrict to the case $d = 3$ (the case $d = 2$ requires a slightly different layer-potential analysis, as outlined in [4, Appendix B]). We assume

$$\kappa(x,t) = \begin{cases} \kappa_0, & x \in \mathbb{R}^d \setminus \overline{D}, \\ \kappa_b \kappa_i(t), & x \in D_i, \end{cases}, \qquad \rho(x,t) = \begin{cases} \rho_0, & x \in \mathbb{R}^d \setminus \overline{D}, \\ \rho_b \rho_i(t), & x \in D_i. \end{cases} \tag{A.5}$$

We denote the outgoing (respectively incoming) Helmholtz Green's functions by $G^{k,+}$ (respectively $G^{k,-}$), defined by

$$G^{k,\pm}(x,y) := -\frac{e^{\pm \mathrm{i}k|x-y|}}{4\pi|x-y|}, \quad x, y \in \mathbb{R}^3, x \neq y, k \in \mathbb{C}.$$

Let $D \in \mathbb{R}^3$ be as in Section 2.1. We introduce the single layer potential $\mathcal{S}_D^{k,\pm} : L^2(\partial D) \to H^1_{\mathrm{loc}}(\mathbb{R}^3)$, defined by

$$\mathcal{S}_D^{k,\pm}[\phi](x) := \int_{\partial D} G^{k,\pm}(x,y)\phi(y)\,\mathrm{d}\sigma(y), \quad x \in \mathbb{R}^3.$$

We observe that $\mathcal{S}_D^{0,+} = \mathcal{S}_D^{0,-} =: \mathcal{S}_D$. Taking the trace on ∂D, it is well-known that $\mathcal{S}_D : L^2(\partial D) \to H^1(\partial D)$ is invertible. We define the basis functions ψ_i and the capacitance coefficients C_{ij} as

$$\psi_i = (\mathcal{S}_D)^{-1}[\chi_{\partial D_i}], \qquad C_{ij} = -\int_{\partial D_i} \psi_j \,\mathrm{d}\sigma,$$

for $i, j = 1, ..., N$. The capacitance matrix C is defined as the matrix $C = (C_{ij})$. Following the steps in Section 4, we can then prove the following result.

Theorem A.2. *Assume that the material parameters are given by* (A.5)*. Then, as* $\delta \to 0$*, the quasifrequencies* $\omega \in Y_t^*$ *to the wave equation* (2.1) *in the subwavelength regime are, to leading order, given by the quasifrequencies of the system of ordinary differential equations*

$$\sum_{j=1}^{N} C_{ij} c_j(t) = \frac{|D_i|\rho_b}{\delta\kappa_b} \frac{1}{\rho_i(t)} \frac{\mathrm{d}}{\mathrm{d}t} \left(\frac{1}{\kappa_i(t)} \frac{\mathrm{d}\rho_i c_i}{\mathrm{d}t} \right) + o(1), \tag{A.6}$$

for $i = 1, ..., N$*.*

References

[1] H. Ammari and B. Davies. A fully coupled subwavelength resonance approach to filtering auditory signals. *Proc. R. Soc. A*, 475(2228):20190049, 2019.

[2] H. Ammari, B. Davies, E. O. Hiltunen, H. Lee, and S. Yu. High-order exceptional points and enhanced sensing in subwavelength resonator arrays. *Studies in Applied Mathematics*, 2020.

[3] H. Ammari, B. Davies, H. Lee, E. O. Hiltunen, and S. Yu. Exceptional points in parity–time-symmetric subwavelength metamaterials. *arXiv preprint arXiv:2003.07796*, 2020.

[4] H. Ammari, B. Fitzpatrick, D. Gontier, H. Lee, and H. Zhang. Minnaert resonances for acoustic waves in bubbly media. *Annales de l'Institut Henri Poincaré C, Analyse non linéaire*, 35(7):1975–1998, 2018.

[5] H. Ammari, B. Fitzpatrick, E. O. Hiltunen, H. Lee, and S. Yu. Honeycomb-lattice minnaert bubbles. *SIAM Journal on Mathematical Analysis*, 52(6):5441–5466, 2020.

[6] H. Ammari, B. Fitzpatrick, H. Kang, M. Ruiz, S. Yu, and H. Zhang. *Mathematical and Computational Methods in Photonics and Phononics*, volume 235 of *Mathematical Surveys and Monographs*. American Mathematical Society, Providence, 2018.

[7] H. Ammari, B. Fitzpatrick, H. Lee, S. Yu, and H. Zhang. Subwavelength phononic bandgap opening in bubbly media. *Journal of Differential Equations*, 263(9):5610–5629, 2017.

[8] H. Ammari, B. Fitzpatrick, H. Lee, S. Yu, and H. Zhang. Double-negative acoustic metamaterials. *Quart. Appl. Math.*, 77(4):767–791, 2019.

[9] H. Ammari, E. O. Hiltunen, and S. Yu. A high-frequency homogenization approach near the dirac points in bubbly honeycomb crystals. *Archive for Rational Mechanics and Analysis*, 238(3):1559–1583, 2020.

[10] H. Ammari, H. Kang, and H. Lee. *Layer potential techniques in spectral analysis.* Number 153. American Mathematical Soc., 2009.

[11] G. Bal, M. Fink, and O. Pinaud. Time-reversal by time-dependent perturbations. *SIAM Journal on Applied Mathematics*, 79(3):754–780, 2019.

[12] E. S. Cassedy. Dispersion relations in time-space periodic media part ii—unstable interactions. *Proceedings of the IEEE*, 55(7):1154–1168, 1967.

[13] A. Cullen. A travelling-wave parametric amplifier. *Nature*, 181(4605):332–332, 1958.

[14] R. Fleury, A. B. Khanikaev, and A. Alu. Floquet topological insulators for sound. *Nature communications*, 7(1):1–11, 2016.

[15] X. Guo, Y. Ding, Y. Duan, and X. Ni. Nonreciprocal metasurface with space–time phase modulation. *Light: Science & Applications*, 8(1):1–9, 2019.

[16] W. Heiss. The physics of exceptional points. *J. Phys. A: Math. Theor.*, 45(44):444016, 2012.

[17] T. T. Koutserimpas and R. Fleury. Electromagnetic waves in a time periodic medium with step-varying refractive index. *IEEE Transactions on Antennas and Propagation*, 66(10):5300–5307, 2018.

[18] T. T. Koutserimpas and R. Fleury. Zero refractive index in time-floquet acoustic metamaterials. *Journal of Applied Physics*, 123(9):091709, 2018.

[19] T. T. Koutserimpas and R. Fleury. Electromagnetic fields in a time-varying medium: Exceptional points and operator symmetries. *IEEE Transactions on Antennas and Propagation*, 2020.

[20] P. Kuchment. *Floquet Theory for Partial Differential Equations.* Number 60 in Operator Theory: Advances and Applications. Birkhäuser Verlag, Basel, 1993.

[21] J. Li, C. Shen, X. Zhu, Y. Xie, and S. A. Cummer. Nonreciprocal sound propagation in space-time modulated media. *Physical Review B*, 99(14):144311, 2019.

[22] J.-L. Lions. Contrôlabilité exacte, perturbations et stabilisation de systèmes distribués. tome 1. *RMA*, 8, 1988.

[23] G. Ma and P. Sheng. Acoustic metamaterials: From local resonances to broad horizons. *Sci. Adv.*, 2(2):e1501595, 2016.

[24] N. W. McLachlan. Theory and application of mathieu functions. *Publisher to the University Geoffrey Cumberlege, Oxford University Press*, 1951.

[25] J. Mendonça and P. Shukla. Time refraction and time reflection: two basic concepts. *Physica Scripta*, 65(2):160, 2002.

[26] F. R. Morgenthaler. Velocity modulation of electromagnetic waves. *IRE Transactions on microwave theory and techniques*, 6(2):167–172, 1958.

[27] L. M. Nash, D. Kleckner, A. Read, V. Vitelli, A. M. Turner, and W. T. Irvine. Topological mechanics of gyroscopic metamaterials. *Proceedings of the National Academy of Sciences*, 112(47):14495–14500, 2015.

[28] H. Nassar, H. Chen, A. Norris, M. Haberman, and G. Huang. Non-reciprocal wave propagation in modulated elastic metamaterials. *Proceedings of the Royal Society A: Mathematical, Physical and Engineering Sciences*, 473(2202):20170188, 2017.

[29] H. Nassar, H. Chen, A. Norris, and G. Huang. Quantization of band tilting in modulated phononic crystals. *Physical Review B*, 97(1):014305, 2018.

[30] A. Ourir and M. Fink. Active control of the spoof plasmon propagation in time varying and non-reciprocal metamaterial. *Scientific reports*, 9(1):1–8, 2019.

[31] S. Raghu and F. D. M. Haldane. Analogs of quantum-hall-effect edge states in photonic crystals. *Physical Review A*, 78(3):033834, 2008.

[32] M. C. Rechtsman, J. M. Zeuner, Y. Plotnik, Y. Lumer, D. Podolsky, F. Dreisow, S. Nolte, M. Segev, and A. Szameit. Photonic floquet topological insulators. *Nature*, 496(7444):196–200, 2013.

[33] D. L. Sounas and A. Alù. Non-reciprocal photonics based on time modulation. *Nature Photonics*, 11(12):774–783, 2017.

[34] L. Wang, R.-Y. Zhang, B. Hou, Y. Huang, S. Li, and W. Wen. Subwavelength topological edge states based on localized spoof surface plasmonic metaparticle arrays. *Opt. Express*, 27(10):14407–14422, May 2019.

[35] J. Wilson, F. Santosa, and P. Martin. Temporally manipulated plasmons on graphene. *SIAM Journal on Applied Mathematics*, 79(3):1051–1074, 2019.

[36] J. Wilson, F. Santosa, M. Min, and T. Low. Temporal control of graphene plasmons. *Physical Review B*, 98(8):081411, 2018.

[37] S. Yves, R. Fleury, T. Berthelot, M. Fink, F. Lemoult, and G. Lerosey. Crystalline metamaterials for topological properties at subwavelength scales. *Nat. Commun.*, 8:16023 EP –, Jul 2017. Article.

[38] S. Yves, R. Fleury, F. Lemoult, M. Fink, and G. Lerosey. Topological acoustic polaritons: robust sound manipulation at the subwavelength scale. *New J. Phys.*, 19(7):075003, 2017.